A proteome analysis of the arsenite response in cultured lung cells: evidence for *in vitro* oxidative stress-induced apoptosis

Andy T. Y. LAU*†, Qing-Yu HE†‡ and Jen-Fu CHIU*†[1]

*Institute of Molecular Biology, The University of Hong Kong, Pokfulam Road, Hong Kong SAR, People's Republic of China, †Open Laboratory of Chemical Biology of the Institute of Molecular Technology for Drug Discovery and Synthesis, The University of Hong Kong, Pokfulam Road, Hong Kong SAR, People's Republic of China, and ‡Department of Chemistry, The University of Hong Kong, Pokfulam Road, Hong Kong SAR, People's Republic of China

Arsenite is well documented as a chemotherapeutic agent capable of inducing cell death. However, the cellular response at the molecular level has not been studied extensively. In the present study, we provide for the first time a proteomic analysis of rat LECs (lung epithelial cells) treated with arsenite, with the aim of identifying defence proteins, probably expressed to protect the cells during the course of arsenic-induced apoptosis. Comparative proteome analysis was conducted on LECs and LECs treated with 40 μM arsenite to identify global changes in their protein expression profiles. Over 1000 protein spots were separated by two-dimensional electrophoresis and visualized by silver staining. Seven proteins changed expression levels significantly and were identified by matrix-assisted laser-desorption ionization–time-of-flight mass spectrometry and database searching. The proteins up-regulated were mostly HSPs (heat-shock proteins) and anti-oxidative stress proteins, including HSP70, aldose reductase, haem oxygenase-1, HSP27, ferritin light chain and αB-crystallin. The glycolytic enzyme glyceraldehyde-3-phosphate dehydrogenase was down-regulated. Pretreatment with the thiol antioxidants glutathione or *N*-acetylcysteine before arsenite insult effectively abrogated the induction of these defence proteins and sustained cell viability, whereas antioxidants were protective only at earlier time points if they were added to cells after arsenite. Taken together, our results demonstrate that high levels of arsenite cause oxidative stress-induced apoptosis.

Key words: apoptosis, arsenite, heat shock protein (HSP), matrix-assisted laser-desorption ionization–time-of-flight mass spectrometry (MALDI–TOF-MS), oxidative stress, reactive oxygen species (ROS).

INTRODUCTION

Arsenic is a well-known carcinogen and possibly acts as a tumour promoter in the process of carcinogenesis [1–4]. Although arsenic has been shown to induce chromosomal aberrations and sister chromatid exchanges when present during DNA replication, the results of genotoxicity studies indicate that it is not mutagenic. It may interfere with the DNA repair system or DNA methylation state, inhibition of p53 and telomerase activities [5–13], oxidative stress, promotion of cell proliferation and signal transduction pathways leading to the activation of transcription factors [14–16]. It has also been shown that arsenic induces DNA damage via the production of ROS (reactive oxygen species) [17].

Paradoxically, high levels of arsenic compounds are also therapeutic agents for treatment of psoriasis, syphilis, rheumatosis and a number of malignant tumours [1]. As a chemotherapeutic agent, arsenic trioxide acts against acute promyelocytic leukaemia, and induces differentiation and apoptosis of malignant cells *in vitro* and *in vivo* [18–20]. However, the mechanisms of these effects have not yet been elucidated. Our previous studies demonstrated a molecular mechanism by which mitogen-activated protein kinase pathways differentially contribute to cell growth regulation and cell death in response to arsenite [21]. A low level (2 μM) of arsenite stimulated the extracellular-signal-regulated kinase signalling pathway and enhanced cell proliferation, whereas a high level (40 μM) stimulated the JNK (c-Jun N-terminal kinase) signalling pathway and induced cell apoptosis. A high level of arsenite has also recently been shown to initiate oxidative stress and telomere erosion, leading to apoptosis [22].

Arsenite-induced stress shares many features similar to heat shock [23]. These include the differential sensitivity of the stress signal pathway to the magnitude of the stress, the activation of the response elements and the protective role of the heat shock response [23]. Oxidative stress arises when ROS are generated, which can react with cellular constituents such as lipids and protein thiols. Depletion of GSH by oxidant then alters the redox status of the cell, resulting in a stressful environment that may play a role in the process of arsenic carcinogenesis [24].

In the present study, we investigate further the transient effects of arsenite in LECs (lung epithelial cells) using a proteomic approach. Proteomics is a powerful tool developed to enhance our study of complex biological systems [25]. This technique has been extensively employed to investigate the proteome response of cells to drugs and other diseases [26,27]. However, to our knowledge, no proteomic study of arsenite has yet been conducted to improve our understanding of cellular response to arsenite. By using comparative proteome analysis between LECs and LECs treated with arsenite, proteins that were differentially expressed were identified by MALDI–TOF-MS (matrix-assisted laser-desorption ionization–time-of-flight mass spectrometry) and database searching. We show that a high concentration of arsenite treatment induced the expression of a group of heat shock

Abbreviations used: αB-C, αB-crystallin; AR, aldose reductase; DAPI, 4,6-diamidino-2-phenylindole; 2-DE, two-dimensional electrophoresis; FLC, ferritin light chain; GAPDH, glyceraldehyde-3-phosphate dehydrogenase; HO-1, haem oxygenase-1; HSP, heat-shock protein; sHSP, small heat shock or stress protein; IEF, isoelectric focusing; JNK, c-Jun N-terminal kinase; LEC, lung epithelial cell; MALDI–TOF-MS, matrix-assisted laser-desorption ionization–time-of-flight mass spectrometry; NAC, *N*-acetylcysteine; ROS, reactive oxygen species.

[1] To whom correspondence should be addressed (email jfchiu@hkucc.hku.hk).

and antioxidative stress proteins, which served to protect the cells against oxidative stress-induced apoptosis exerted by arsenite.

EXPERIMENTAL

Materials and reagents

Sodium arsenite, NAC (*N*-acetylcysteine) and GSH were purchased from Sigma (St. Louis, MO, U.S.A.). PlusOne 2-D Clean-Up kit was purchased from Amersham Biosciences (Uppsala, Sweden). DAPI (4,6-diamidino-2-phenylindole) was purchased from Roche (Mannheim, Germany). All other general chemicals were purchased from Amersham Biosciences and Sigma. Antibodies used for Western blot were purchased from Sigma, Upstate Biotechnology (Lake Placid, NY, U.S.A.), StressGen Biotechnologies (Victoria, BC, Canada) and Santa Cruz Biotechnology (Santa Cruz, CA, U.S.A.).

Cell culture

A rat LEC line was isolated and characterized by Li et al. [24]. Cells were routinely grown at 37 °C in 95 % air/5 % CO_2 using F-12 nutrient, supplemented with 2 mmol/l glutamine, 100 units/ml penicillin, 100 μg/ml streptomycin (Gibco BRL, Grand Isle, NY, U.S.A.) and 10 % (v/v) newborn bovine serum (JRH Bioscience, Lenexa, KS, U.S.A.).

Arsenite treatment

Cells were grown to 75 % confluence and then were either sham-exposed or treated with different concentrations of $NaAsO_2$. Cells were pretreated with GSH or NAC for 1 h before the addition of arsenite.

Quantification of apoptotic death

To detect apoptosis, nuclear staining was performed using 1 μg/ml DAPI, and cells were analysed with a fluorescence microscope. Apoptotic cells were identified by morphology and by condensation and fragmentation of their nuclei. The percentage of apoptotic cells was calculated as the ratio of apoptotic cells to total cells counted, multiplied by 100. Three separate experiments were conducted and at least 300 cells were counted for each experiment.

Protein quantification

Protein concentrations in all experiments were determined by Bradford's method using the Bio-Rad protein assays with reference to the standard curve of BSA [28].

Cell lysate preparation and conditions of 2-DE (two-dimensional electrophoresis) and Western blot

After treatment, cells were washed three times with ice-cold PBS, scraped into centrifuge tube and harvested by centrifugation at 1000 ***g*** for 5 min at 4 °C.

For 2-DE analysis, cell pellets were lysed in lysis buffer [8 M urea and 4 % (w/v) CHAPS], incubated on ice for 30 min and centrifuged at 16 000 ***g*** for 5 min at 4 °C. The supernatant was saved and then purified further by the PlusOne 2-D Clean-Up kit, in accordance with the manufacturer's instructions. The purified samples were finally redissolved in rehydration buffer (8 M urea and 2 % CHAPS), aliquoted into several tubes and stored at − 80 °C after protein quantification. 2-DE was performed with Amersham Biosciences IPGphor IEF (isoelectric focusing) and Hoefer SE 600 electrophoresis unit in accordance with the manufacturer's instructions. Briefly, 80 μg of cleaned-up cell extract was mixed with 250 μl of rehydration buffer containing 8 M urea, 2 % CHAPS, 0.28 % (w/v) dithiothreitol and 0.5 % (v/v) Pharmalyte (Amersham Biosciences). Rehydration was performed with precasted 13 cm IPG strips for 12 h under a low voltage of 30 V, 50 μA per strip at 20 °C. IEF was run following a stepwise voltage increase procedure: 500 and 1000 V for 1 h each and then 64 000 Vh. After IEF, the strips were subjected to two-step equilibration of 15 min each in the equilibration buffer [6 M urea, 30 % (v/v) glycerol, 2 % (w/v) SDS and 50 mM Tris/HCl, pH 8.8] with 1 % dithiothreitol for the first step and 2.5 % (w/v) iodoacetamide for the second step. The strips were then loaded on to the second dimension 12.5 % SDS/polyacrylamide gel, positioned into the gel with an overlay of warm agarose sealing solution [0.5 % (w/v) agarose and 0.002 % (w/v) Bromophenol Blue in 1 × SDS running buffer] and resolved at 15 mA/gel for 15 min. Separation continued at 30 mA/gel until the dye front nearly reached the bottom.

For Western-blot analysis, equal amounts of proteins were fractionated on SDS/polyacrylamide gel and transferred on to PVDF membranes. The membranes were blocked with 5 % (w/v) non-fat dry milk in PBS containing 0.05 % Tween 20 (PBST) and probed with various primary antibodies. After incubation with secondary antibodies, immunoblots were visualized with the ECL® detection kit (Amersham Biosciences). For reprobing the membrane with another antibody, the membrane was stripped in 2 % SDS, 0.1 % 2-mercaptoethanol and 50 mM Tris/HCl (pH 6.8) and boiled at 50 °C for 30 min.

Silver staining

All solutions were made with Milli-Q water. The gels were fixed overnight in fixing solution [40 % (v/v) ethanol and 10 % (v/v) acetic acid], and then incubated in sensitizing solution [30 % ethanol, 6.8 % (w/v) sodium acetate and 0.2 % sodium thiosulphate] for 30 min. The gels were washed three times with Milli-Q water for 10 min each, and stained in silver solution (0.25 % silver nitrate and 0.0148 % formaldehyde) for 30 min. They were again washed twice with Milli-Q water for 1 min each and developed for 10 min in a developing solution [2.5 % (w/v) sodium carbonate and 0.0074 % formaldehyde]. The developing reaction was terminated by incubation in stopping solution (1.46 % EDTA) for 10 min, and the stained gels were finally washed three times with Milli-Q water for 5 min each.

Image acquisition and analysis

The stained gels were scanned using an ImageScanner (Amersham Biosciences) operated by the software program LabScan 3.00. Intensity calibration was performed with an intensity step wedge before gel image capture. Image analysis was performed with ImageMaster 2D Elite software 4.01. Image spots were initially detected, matched and then manually edited. The intensity volume of each spot was processed by background subtraction and total spot volume normalization, and the resulting spot volume percentage was used for comparison. Only significantly up- or down-regulated spots ($\pm$ over 2-fold) or spots which appeared or disappeared were selected for analysis with MS.

Tryptic in-gel digestion

Protein spots were excised and transferred to siliconized 1.5 ml Eppendorf tubes. Gel chips were destained in a freshly prepared 1:1 mixture solution of 30 mM potassium ferricyanide

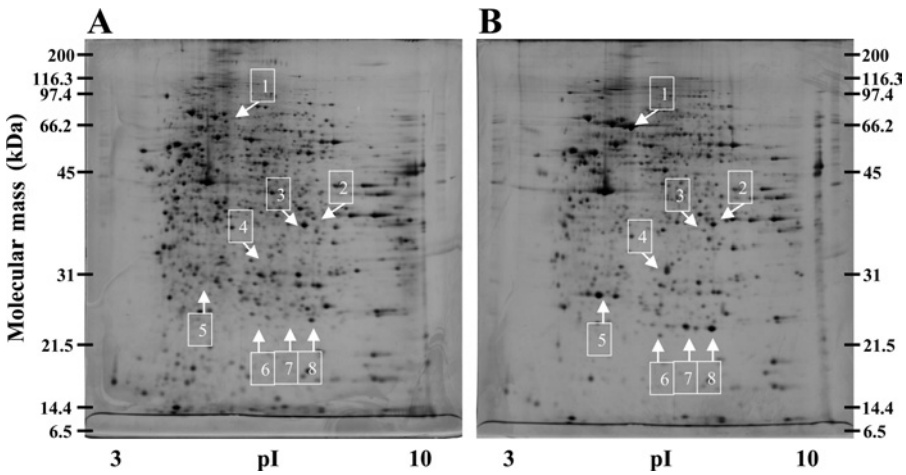

Figure 1 Representative gel images of LECs treated with or without 40 μM arsenite for 24 h visualized by two-dimensional gel (12.5%) and silver staining

(**A**) Control LECs and (**B**) LECs treated with 40 μM arsenite. Differentially expressed proteins are numbered from 1 to 8 and indicated by arrows. The protein spots were excised, in-gel-digested with trypsin and analysed by MALDI–TOF-MS.

and 100 mM sodium thiosulphate and then equilibrated in 50 mM ammonium bicarbonate until pH 8.0 was reached. After dehydrating with acetonitrile and drying in a SpeedVac, the gels were rehydrated in a minimal volume of trypsin solution (10 μg/ml in 25 mM NH_4HCO_3) and incubated overnight at 37 °C. The digest was then applied on to a sample plate and coated with matrix (α-cyano-4-hydroxycinnamic acid). If necessary, the in-gel digest was extracted subsequently with 50 and 80 % (v/v) acetonitrile, and then concentrated and desalted by Ziptip before being applied on to the sample plate.

MALDI–TOF-MS analysis and protein identification

Tryptic peptide mass spectra were obtained using a Voyager-DE STR MALDI–TOF mass spectrometer (Applied Biosystems, Foster City, CA, U.S.A.). The instrument was set in reflector mode with 175 ns delay extraction time, 60–65 % grid voltage and 20 k accelerating voltage. To acquire the spectra with mass ranging from 0.6 to 2.5 kDa, 250 laser shots per spectrum were used. The trypsin autolytic fragment peaks (906.5049, 1153.5741 and 2163.0570) served as internal standards for mass calibration. Protein identification was performed by searching in NCBInr protein database using MS-Fit (http://prospector.ucsf.edu/). The criteria for searching were (i) 25 p.p.m. or better mass accuracy, (ii) at least four matching peptide masses, and (iii) match between molecular mass and pI, and estimated values from gels. Species search was limited to *Rattus norvegicus*.

RESULTS

Proteome profiles between LECs and LECs treated with 40 μM arsenite

After treatment with arsenite, LEC extracts were isolated and applied to 2-DE and proteins visualized by silver staining. To minimize gel to gel variation, two-dimensional gels were run three times for each sample. Figure 1 shows the representative gel images for normal control cells (Figure 1A) and LECs treated with 40 μM arsenite for 24 h (Figure 1B). More than 1000 spots were detected in a gel with molecular mass ranging from 6 to 200 kDa and pI values between 3 and 10. Comparison of spot volume was made between the samples with the ImageMaster program. Arsenite (40 μM) treatment produced significant differences in at least eight areas.

Protein identification

A high level of arsenite altered the protein profile in LECs (Figure 1). Protein spots that displayed significant differences (up- or down-regulated spots over 2-fold or spots which appeared or disappeared) were cut out and subjected to trypsin digestion, MALDI–TOF mass spectra measurement and database searching. Table 1 summarizes the identified proteins in the eight areas and their alterations between normal control and 40 μM arsenite-treated cells. In general, the obtained sequence coverage percentage ranged from 22 to 50 % of full-length protein at 25 p.p.m. The proteins up-regulated were HSPs (heat-shock proteins), including HSP70, HO-1 (haem oxygenase-1; HSP32), HSP27 and αB-C (αB-crystallin), and antioxidative stress proteins such as AR (aldose reductase) and FLC (ferritin light chain). The glycolytic enzyme GAPDH (glyceraldehyde-3-phosphate dehydrogenase) was down-regulated. Spots 7 and 8 were both αB-C, but spot 7 was the phosphorylated form of αB-C. This was evidenced by the tryptic peptide mass spectrum for differences in peptide masses of 0.08 kDa that were not found in spot 8 (results not shown). Expression of these seven proteins in basal and arsenite-treated cells was further examined by immunoblotting, which showed a similar trend of induction or repression as they appeared in two-dimensional gels (Figure 2).

Time- and concentration-dependent expression of individual stress proteins induced by high levels of arsenite

Since a high level of arsenite altered the proteome profile and induced the expression of stress proteins within 24 h, we attempted to determine the time of induction/repression of individual proteins, throughout a 24 h time interval. On this occasion, we used 40 μM arsenite and the intermediate dose (20 μM) to address the time and concentration effects on the protein expression profile. As shown in Figure 3(A), 20 μM arsenite treatment altered the proteome profile in much the same way as 40 μM arsenite treatment (Figure 3B). However, GAPDH was not altered within the 24 h interval, and the induction of all other proteins with 20 μM arsenite treatment was also somewhat weaker when

Table 1 Identification of proteins differentially expressed between LECs and LECs treated with 40 μM arsenite for 24 h

Spot no./identified protein	NCBI accession no.	Mass (kDa)/pI	Coverage (%)*	Volume (%) (means ± S.D.) Untreated	Volume (%) (means ± S.D.) Treated	Fold difference†	Function
1. HSP70	27704462	70.2/5.6	41	ND‡	0.777 ± 0.104	N/A§	Chaperone
2. AR	27465603	36.2/7.1	32	0.177 ± 0.00493	0.604 ± 0.0517	+ 3.4	Glucose reduction
3. GAPDH	8393418	35.8/8.1	22	0.698 ± 0.00985	0.137 ± 0.0315	−5.1	Glycolysis
4. HO-1	6981032	33/6.1	40	ND	0.788 ± 0.0936	N/A	Haem cleavage
5. HSP27	1170367	22.9/6.1	46	0.0870 ± 0.00458	0.982 ± 0.0566	+ 11.3	Chaperone
6. FLC	2119695	20.8/6.0	33	0.0217 ± 0.00950	0.172 ± 0.0168	+ 7.9	Intracellular iron regulation
7. αB-C (phosphorylated)	16905067	20/6.8	49	ND	0.789 ± 0.0481	N/A	Chaperone
8. αB-C	16905067	20/6.8	50	0.381 ± 0.0167	1.115 ± 0.0785	+ 2.9	Chaperone

* Sequence coverage (%) of full-length protein at 25 p.p.m.
† Average expression level in arsenite-treated cells compared with LECs from three independent analyses (+, increase; −, decrease).
‡ ND, non-detectable.
§ N/A, not applicable.

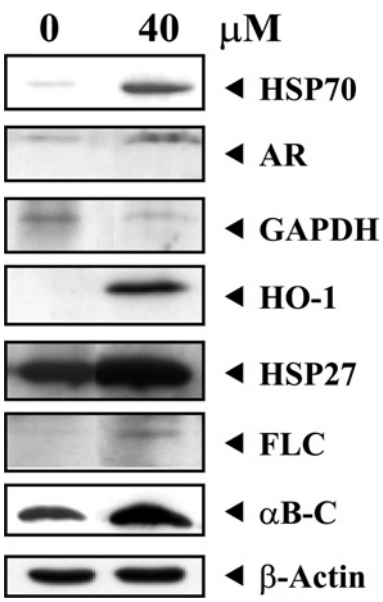

Figure 2 Western-blot analysis of differentially expressed proteins following 40 μM arsenite treatment

LECs were treated with or without 40 μM sodium arsenite for 24 h. Total cellular proteins were subjected to Western-blot analysis for the detection of seven proteins (HSP70, AR, GAPDH, HO-1, HSP27, FLC and αB-C). The same blot was also reprobed with monoclonal anti-β-actin antibody to monitor the loading difference. The results are representative of three independent experiments.

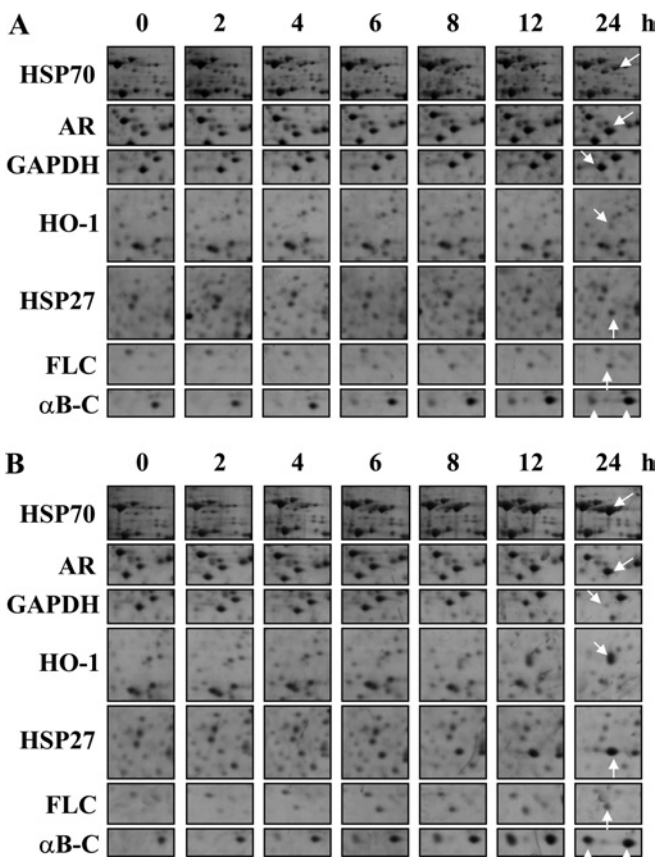

Figure 3 Time-course experiment on LECs treated with high and intermediate levels of arsenite for 24 h showed reproducible changes in proteome profile compared with control

Cells were challenged with 20 or 40 μM arsenite, harvested at 0, 2, 4, 6, 8, 12 and 24 h and subjected to 2-DE analyses. Protein expression profiles of seven proteins in basal and arsenite-treated cells throughout the 24 h time intervals were assessed by 2-DE analyses and shown in montage view. Cells with (**A**) 20 μM and (**B**) 40 μM arsenite exposure. The results are representative of three independent experiments.

compared with 40 μM arsenite treatment. Table 2 summarizes the spot volume of seven proteins throughout the 24 h time interval and Table 3 summarizes the initial time of induction or repression of these proteins in LECs treated with 40 μM arsenite for 24 h.

Induction of stress proteins by arsenite is modulated by intracellular GSH in LECs

Several studies have suggested that the level of intracellular GSH is an important determinant for the biological effects of arsenite [29]. Our previous studies [24] have shown that the depletion of GSH by buthionine sulphoximine potentiated the effects of arsenite, whereas pretreatment of GSH protected the cells against oxidative stress. To investigate the protective role of intracellular GSH in the induction of stress proteins by arsenite in LECs, we tested the effect of pretreatment with GSH and NAC. NAC is

Table 2 Time-course experiment on LECs treated with high and intermediate levels of arsenite for 24 h

Spot no./identified protein	Arsenite (μM)	Volume (%) (mean)*						
		0 h	2 h	4 h	6 h	8 h	12 h	24 h
1. HSP70	20	ND	ND	0.125	0.253	0.280	0.340	0.402
	40	ND	ND	0.138	0.395	0.581	0.713	0.867
2. AR	20	0.178	0.189	0.201	0.378	0.486	0.502	0.603
	40	0.181	0.192	0.203	0.382	0.490	0.510	0.620
3. GAPDH	20	0.699	0.700	0.696	0.697	0.696	0.694	0.695
	40	0.702	0.695	0.694	0.686	0.682	0.484	0.147
4. HO-1	20	ND	ND	ND	ND	0.059	0.066	0.201
	40	ND	ND	ND	0.048	0.211	0.515	0.802
5. HSP27	20	0.087	0.112	0.128	0.193	0.208	0.267	0.332
	40	0.088	0.169	0.255	0.416	0.512	0.801	0.994
6. FLC	20	0.024	0.035	0.073	0.098	0.105	0.111	0.124
	40	0.025	0.052	0.109	0.147	0.158	0.162	0.187
7. αB-C (phosphorylated)	20	ND	ND	0.079	0.152	0.262	0.356	0.416
	40	ND	0.029	0.146	0.203	0.504	0.819	0.829
8. αB-C	20	0.391	0.404	0.412	0.497	0.712	0.747	0.764
	40	0.393	0.408	0.428	0.698	0.735	1.023	1.147

* Data are derived from Figures 3(A) and 3(B) and expressed as mean values for three independent analyses.

Table 3 Summary of the time of induction/repression of differentially expressed proteins in LECs treated with 40 μM arsenite for 24 h and the critical time after which addition of NAC to arsenite-treated cells fails to restore the protein expression level to that of control

Spot no./identified protein	Time of onset of induction/repression (h)*	Critical time for failure of NAC effect (h)†
1. HSP70	4	2
2. AR	6	2
3. GAPDH	12	8
4. HO-1	8	6
5. HSP27	2	4
6. FLC	2	4
7. αB-C (phosphorylated)	4	4
8. αB-C	6	2

* Data are derived from Figure 3(B).
† Data are derived from Figure 6(A).

routinely used in human patients to overcome lethal oxidative stress caused by acetaminophen overdose. We used 40 μM arsenite to treat the cells, as this concentration induced all stress proteins and produced obvious proteome changes. Pretreatment with $\geqslant$10 mM NAC or GSH effectively inhibited the induction of stress proteins and produced a similar proteome profile to that of the control cells (Figures 4A and 4C). The corresponding spot volume of seven proteins is shown in Table 4. Western-blot analyses of pro-apoptotic protein Bax and procaspase 3 levels (Figures 4B and 4D) showed that pretreatment with 20 mM NAC or GSH effectively suppressed the Bax expression and pro-caspase 3 activation in LECs treated with 40 μM arsenite and also inhibited arsenite-induced apoptosis (Figure 5).

Arsenite-induced apoptosis is correlated with oxidative stress

To show further that arsenite-induced apoptosis in LECs is due to oxidative stress, LECs were exposed to sodium arsenite (5, 10, 20 or 40 μM) for 24 h in the absence or presence of NAC (20 mM). We used 20 mM NAC instead of GSH, as NAC seems to be a better antioxidant when compared with GSH. NAC was added 1 h before the addition of sodium arsenite. Nuclear staining was performed using DAPI, and cells were analysed with a fluorescence microscope. Arsenite induced massive apoptosis in LECs (Figure 5A, upper right panel). Pretreatment with NAC before arsenite insult effectively protected the cells against oxidative stress-induced apoptosis by arsenite (Figure 5A, lower right panel). In the absence of NAC protection, the cell death caused by arsenite was dose-dependent (Figure 5B).

Induction of individual differentially expressed proteins by 40 μM arsenite can only be inhibited by NAC at certain time points

To investigate whether NAC can inhibit the induction of stress proteins several hours after treatment with arsenite, LECs were exposed to sodium arsenite (40 μM) in the absence or presence of NAC (20 mM). NAC was added before ($-$1 h), at the same time (0 h) or at various time points after arsenite treatment. Sodium arsenite was added at time 0 h. After 24 h treatment with arsenite, whole cell lysates were prepared. As shown in Figure 6(A), addition of NAC at $-$1 h (pretreatment) before arsenic insult or at the same time (0 h) effectively countered the effect of arsenite, and the proteome profiles of control cells and experimental cells were the same. When NAC was added 2 h after arsenite treatment or at later time points, the induction or suppression of specific stress proteins began to show an impact on the proteome profile (the corresponding spot volume of seven proteins is shown in Table 5). On the basis of the results from Table 5, Table 3 also summarizes the critical time points when the addition of NAC to arsenite-treated cells first failed to maintain the protein expression level at the control level. The results of DAPI staining for cell apoptosis were consistent with the results of 2-DE analyses. Within 4 h after treatment of arsenite, NAC can protect more than 70 % of cells from cell death. However, NAC gives little protection if added to the cells 6 h after arsenite treatment. Addition of NAC at later time points failed to protect the cells against apoptosis, and cell apoptosis compared with the control cells increased consistently (Figure 6B).

DISCUSSION

To elucidate the general biological effects of arsenic, we concentrated on tervalent state arsenite (AsO_2^-) and studied its effect

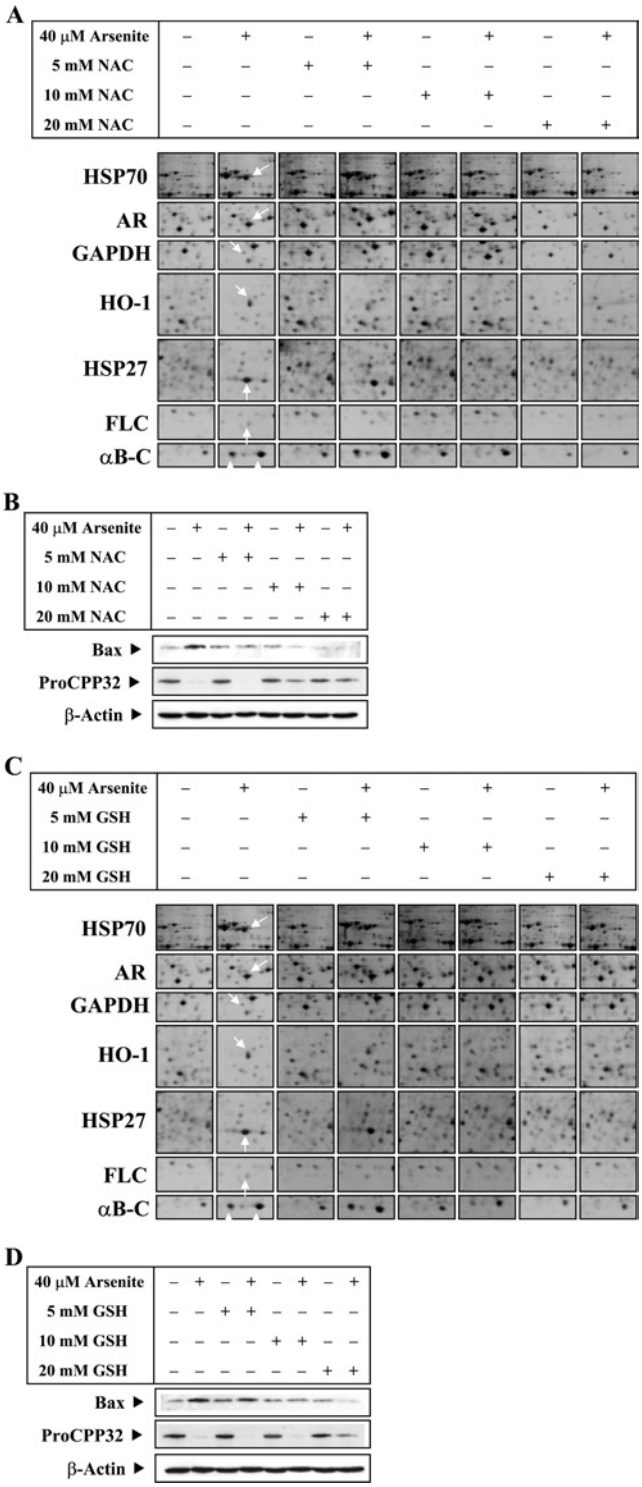

Figure 4 Induction of differentially expressed proteins by a high level of arsenite is inhibited by NAC or GSH

LECs were exposed to sodium arsenite (40 μM) in the absence or presence of NAC (5, 10 or 20 mM) or GSH (5, 10 or 20 mM) (pH adjusted to 7.6). NAC and GSH were added 1 h before the addition of sodium arsenite. LECs were also treated with various concentrations of NAC and GSH alone. After treatment for 24 h, cells were lysed and whole cell lysate was prepared. Effects of NAC (**A**) and GSH (**C**) on protein expression profiles of seven proteins in basal and arsenite-treated cells were assessed by 2-DE analyses and shown in montage view. (**B**, **D**) Western-blot analyses for the detection of Bax and procaspase 3, using anti-Bax and anti-procaspase 3 antibodies respectively and monoclonal anti-β-actin antibody to monitor the loading difference. (**B**) The corresponding Western-blot analysis of (**A**). (**D**) The corresponding Western-blot analysis of (**C**). The results are representative of three independent experiments.

on LECs by proteomics. High levels of arsenite exposure have been shown to cause apoptosis [21,22]. We show that treatment of LECs with 40 μM arsenite produced significant changes in at least eight areas on two-dimensional gel. Among them, the up-regulated proteins can be classified as heat shock or stress proteins, which have antioxidative stress/chaperone functions. For some of these individual proteins, induction occurred as early as 2 or 4 h, whereas other proteins were only expressed later. This showed the dynamics of protein expression in cells battling for survival from apoptosis. Significantly, we show that the proteome profile with 20 μM arsenite treatment is similar to that for 40 μM arsenite treatment. However, GAPDH was not altered throughout the 24 h and the induction of other proteins with 20 μM arsenite treatment was somewhat less pronounced when compared with 40 μM arsenite treatment. The stress signal exerted by 20 μM arsenite was also less catastrophic when compared with 40 μM arsenite insults. It is desirable to conduct further studies to delineate the proteome changes of the 20 μM arsenite-treated cells. Nevertheless, our results support our previous findings that different doses of arsenite may activate different streams of signalling pathways [21].

The up-regulation of HSP stress proteins by the cells after 40 μM arsenite treatment is a cellular-protective response. The HSPs comprise a group of highly conserved, abundantly expressed proteins with diverse functions and are also known as molecular chaperones. HSPs fall into six families: HSP110, HSP90, HSP70, HSP60, sHSPs (small heat shock or stress proteins) and the immunophilins [30,31]. In the present study, we demonstrated the induction of the HSP70 and sHSP families of stress proteins by 40 μM arsenite.

HSP27 and αB-C belong to the sHSP family. They are expressed constitutively in cells, and their expression is increased in response to various types of stress, including increased temperatures, toxic metals, drugs and oxidants. They exist mainly as oligomers of 8–40 monomers, which display chaperone-like activity, serving as a site where unfolding proteins may bind and refold. The refolding process is ATP- and HSP70-dependent and protects the cell against oxidative stress and apoptosis. Under stress conditions, these large oligomers dissociate into small oligomers as a result of phosphorylation by kinases [32]. Small oligomers of sHSPs can also influence the organization of the microfilaments, such as binding to F-actin [33,34]. Recently, HSP27 has been shown to prevent apoptosis by regulating the activation of the phosphoinositide 3-kinase/protein kinase B pathway [35] and to inhibit cytochrome *c*-dependent activation of procaspase 9 [36]. αB-C has also been shown to be a negative regulator of apoptosis by inhibiting the autocatalytic maturation of caspase 3 [37]. sHSPs can also decrease the intracellular level of ROS by modulating the metabolism of glutathione to maintain it in a reduced state [38]. In the present study, the up-regulation of HSP27 and αB-C appeared to protect the cell against oxidative stress triggered by high levels of arsenite.

Apart from sHSPs, HSP70 also was induced by 40 μM arsenite in LECs. HSP70 is part of the HSP70 family, whose members act as molecular chaperones and are involved in many cellular functions such as protein folding, transport, maturation and degradation. They recognize and bind to nascent polypeptide chains as well as partially folded intermediates of proteins to prevent their aggregation and misfolding. HSP70 can also reduce JNK activity by increasing the rate of its dephosphorylation [39] and binding to JNK to prevent its phosphorylation by upstream kinases [40]. HSP70 subsequently inhibits the apoptotic cascades transduced by JNK. The HSP70 family has also been shown to inhibit cytochrome *c* release and to suppress the activity of caspases [41,42].

Table 4 Summary of induction of differentially expressed proteins by 40 μM arsenite and antioxidants

	Volume (%) (mean)*													
			NAC						GSH					
40 μM arsenite . . .	−	+	−	+	−	+	−	+	−	+	−	+	−	+
5 mM antioxidant . . .	−	−	+	+	−	−	−	−	+	+	−	−	−	−
10 mM antioxidant . . .	−	−	−	−	+	+	−	−	−	−	+	+	−	−
20 mM antioxidant . . .	−	−	−	−	−	−	+	+	−	−	−	−	+	+
1. HSP70	ND	0.789	ND	0.720	ND	ND	ND	ND	ND	0.753	ND	ND	ND	ND
2. AR	0.177	0.612	0.173	0.631	0.171	0.413	0.169	0.167	0.178	0.623	0.172	0.418	0.174	0.412
3. GAPDH	0.697	0.142	0.702	0.468	0.699	0.685	0.691	0.696	0.698	0.453	0.691	0.689	0.695	0.697
4. HO-1	ND	0.798	ND	0.708	ND	ND	ND	ND	ND	0.802	ND	ND	ND	ND
5. HSP27	0.086	0.992	0.088	0.988	0.085	0.084	0.081	0.083	0.087	0.990	0.083	0.172	0.081	0.083
6. FLC	0.023	0.179	0.025	0.173	0.021	0.018	0.019	0.020	0.024	0.181	0.021	0.060	0.019	0.022
7. αB-C (phosphorylated)	ND	0.793	ND	0.788	ND	0.209	ND	ND	ND	0.792	ND	0.410	ND	ND
8. αB-C	0.372	1.141	0.384	1.138	0.382	0.401	0.371	0.373	0.391	1.129	0.374	0.611	0.378	0.381

* Data are derived from Figures 4(A) and 4(C) and expressed as mean values for three independent analyses.

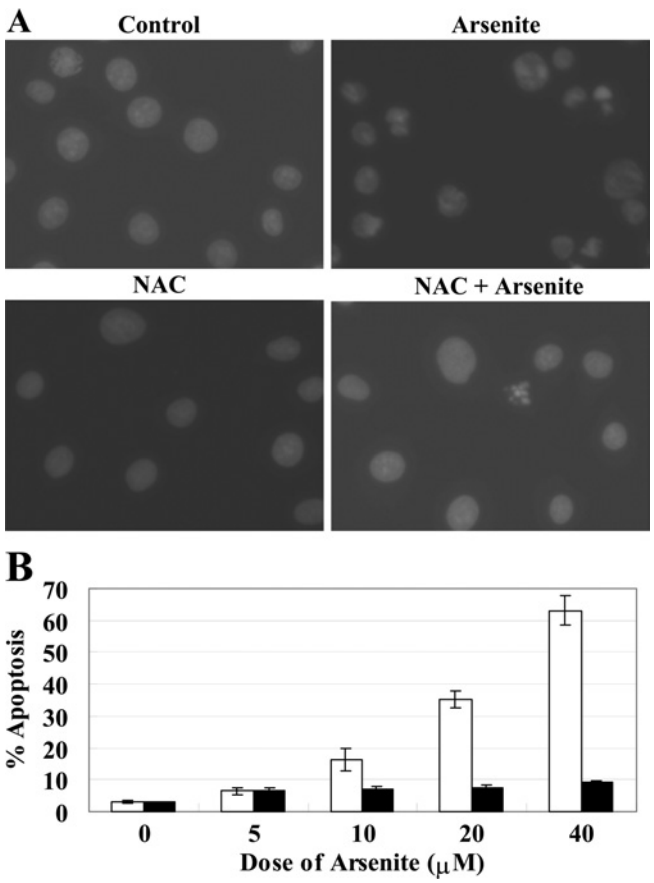

Figure 5 Arsenite-induced apoptosis is correlated with oxidative stress

LECs were exposed to sodium arsenite (5, 10, 20 or 40 μM) for 24 h in the absence or presence of NAC (20 mM). NAC was added 1 h before the addition of sodium arsenite. Nuclear staining was performed using 1 μg/ml DAPI and cells were analysed with a fluorescence microscope. (**A**) Representative morphological changes of control LEC, pretreated with 20 mM NAC alone and LEC treated with 40 μM arsenite with or without pretreatment with 20 mM NAC are shown. Apoptotic cells were identified by morphology and by condensation and fragmentation of their nuclei. Arsenite induced massive apoptosis in LEC (upper right panel). Pretreatment with NAC before arsenite insult effectively protected the cells against oxidative stress-induced apoptosis by arsenite (lower right panel). (**B**) Arsenite induced apoptosis in a dose-dependent manner and this effect can be countered by 20 mM NAC pretreatment. The percentage of apoptotic cells was calculated as the ratio of apoptotic cells to total cells counted, multiplied by 100. Black bars indicate NAC pretreatment. Results are expressed as means $\pm$ S.D. for triplicate samples and reproducibility was confirmed in three separate experiments.

An increase in ROS levels can perturb the cell redox status, thereby producing damage to lipids, proteins and DNA, and eventually cell death. AR, a member of the aldoketoreductase family, acts as an antioxidative stress protein under oxidative stress conditions by metabolizing several aldehyde product compounds including 4-hydroxy *trans*-2-nonenal, a major toxic product of lipid peroxidation as a result of arsenite insult [43]. Therefore the up-regulation of AR by 40 μM arsenite treatment is expected. Also, when cell redox status is perturbed by ROS, the cells correct the systems to maintain the state of redox balance. HO-1 and FLC were up-regulated significantly after the cells were treated with 40 μM arsenite. HO-1 (HSP32) belongs to the sHSP family, a family of microsomal enzymes that cleave haem to produce biliverdin, inorganic iron and carbon monoxide. HO-1 is a stress protein and its activity is highly inducible in response to numerous stimuli, including haem, heavy metals and hormones. Increased levels of HO-1 can be used as an indication of exposure to oxidative stress [44]. Biliverdin and its product bilirubin play an important role in protecting cells by acting as free radical scavengers [45].

Ferritins regulate iron metabolism. Mammalian ferritins consist of 24 subunits made up of two types of polypeptide chains (ferritin heavy chains and FLCs) [46]. The most prominent role of mammalian ferritins is to provide iron-buffering capacity in the cells. To examine oxidative stress, Cairo et al. [47] showed that ROS induces a 6-fold increase in ferritin expression in rat livers, because it is directly involved in the transcriptional and post-transcriptional activation of this gene through inhibition of iron regulatory factor binding activity. Similarly, our results show that 40 μM arsenite induced an 8-fold increase in the FLC protein level. Clearly, the cleavage of haem by HO-1 produced an increase in intracellular free iron levels. The increase in cellular iron pool induces ferritin gene transcription in an attempt to limit iron bioavailability. In the present study, GAPDH was down-regulated in cells treated with 40 μM arsenite at 24 h. Recent studies have revealed that GAPDH displays diverse non-glycolytic functions, depending on its subcellular localization. Previous studies have demonstrated that the overexpression of GAPDH and its subsequent nuclear translocation are probably implicated in the initiation of apoptotic cascades [48]. In contrast, our results suggest that cells committed apoptosis as a result of a reduction in glycolysis, manifested by the repression of GAPDH.

Western-blot analyses showed that the levels of Bax and procaspase 3 in 40 μM arsenite-treated cells at 24 h were significantly increased and activated, indicating that the cells were

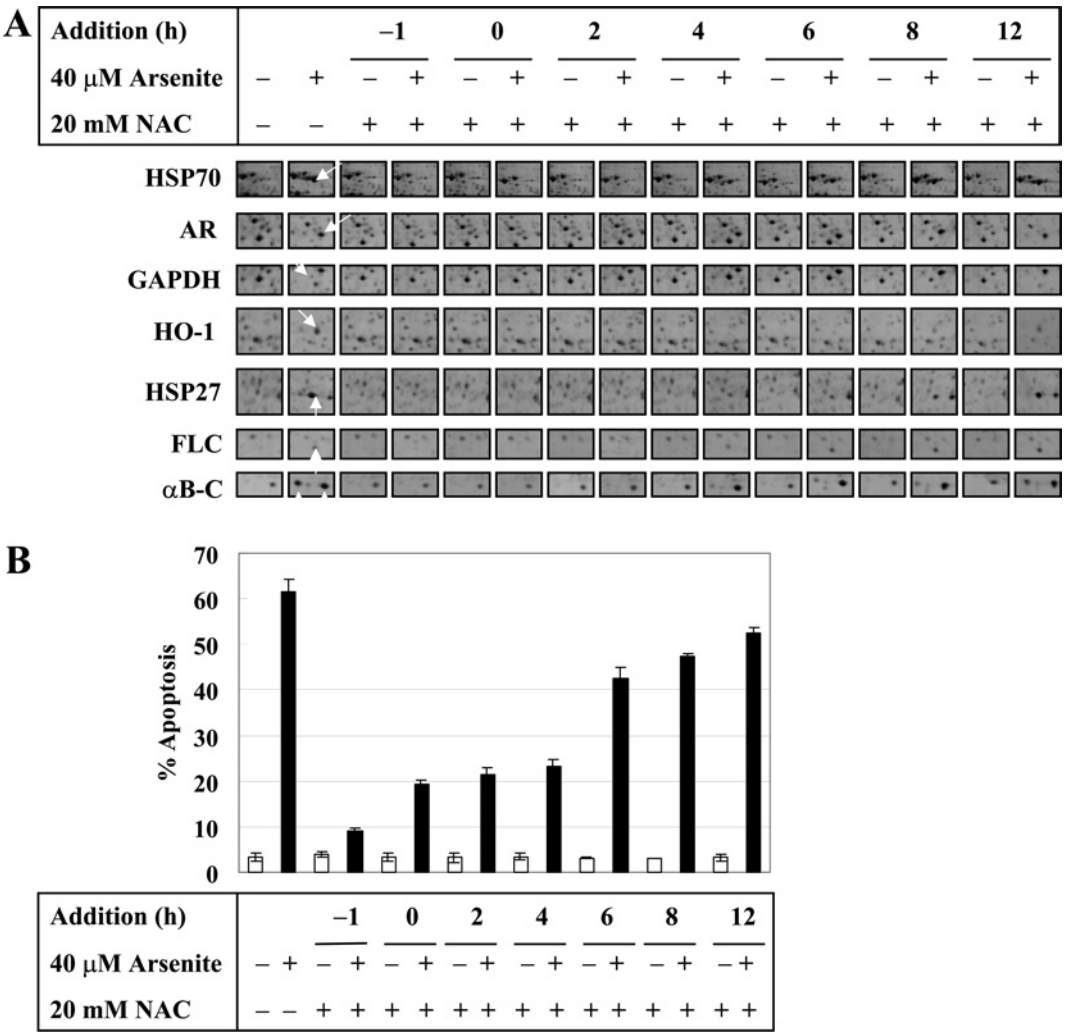

Figure 6 Induction of individual differentially expressed proteins by a high level of arsenite can be inhibited by NAC at unique specific time points

LECs were exposed to sodium arsenite (40 μM) in the absence or presence of NAC (20 mM). NAC was added before (−1 h), at the same time (0 h) or at various later time points and sodium arsenite was added at time 0 h. LECs were also treated with NAC alone. After 24 h of arsenite treatment, cells were lysed and whole cell lysate was prepared. (**A**) Effects of NAC on protein expression profiles of seven proteins in basal and arsenite-treated cells were assessed by 2-DE analyses and shown in montage view. (**B**) The corresponding DAPI staining of (**A**) for the determination of apoptotic cells. Nuclear staining was performed using 1 μg/ml DAPI, and apoptotic cells were analysed with a fluorescence microscope. Black bars indicate arsenite treatment. Results are expressed as means ± S.D. for triplicate samples and reproducibility was confirmed in three separate experiments.

Table 5 Summary of induction of differentially expressed proteins by 40 μM arsenite and NAC at specific time points

	Volume (%) (mean)*															
			−1 h		0 h		2 h		4 h		6 h		8 h		12 h	
40 μM arsenite . . .	−	+	−	+	−	+	−	+	−	+	−	+	−	+	−	+
20 mM NAC . . .	−	−	+	+	+	+	+	+	+	+	+	+	+	+	+	+
1. HSP70	ND	0.779	ND	ND	ND	ND	ND	0.140	ND	0.630	ND	0.681	ND	0.713	ND	0.757
2. AR	0.175	0.609	0.170	0.174	0.178	0.176	0.177	0.308	0.176	0.581	0.174	0.589	0.172	0.595	0.171	0.607
3. GAPDH	0.693	0.139	0.695	0.691	0.699	0.690	0.697	0.694	0.699	0.693	0.694	0.690	0.695	0.482	0.697	0.136
4. HO-1	ND	0.801	ND	ND	ND	ND	ND	ND	ND	ND	ND	0.123	ND	0.472	ND	0.603
5. HSP27	0.082	0.973	0.085	0.083	0.081	0.079	0.086	0.090	0.083	0.173	0.087	0.238	0.082	0.493	0.085	0.964
6. FLC	0.025	0.173	0.021	0.024	0.021	0.023	0.022	0.025	0.021	0.062	0.019	0.129	0.022	0.148	0.019	0.169
7. αB-C (phosphorylated)	ND	0.791	ND	ND	ND	ND	ND	ND	ND	0.104	ND	0.213	ND	0.382	ND	0.780
8. αB-C	0.381	1.138	0.371	0.374	0.378	0.382	0.382	0.598	0.377	0.793	0.382	0.831	0.375	0.974	0.379	1.110

* Data are derived from Figure 6(A) and expressed as mean values for three independent analyses.

undergoing apoptosis. To investigate whether the antioxidant was still able to protect the cells after arsenite treatment and to identify the relevant time points for protection, we treated the cells with arsenite and added the antioxidant at a later time. Pretreatment with antioxidant 1 h before arsenite challenge effectively blocked the expression of stress proteins. The expression of stress proteins was also inhibited when arsenite and antioxidant were added to the cells at the same time. However, if antioxidant was added at later time points, the expression of stress proteins remained uninhibited and cell viability began to decrease. Some of the stress proteins were also more critical than others. The appearance of stress proteins may signal one of two possible outcomes. In some cases, the stress proteins can render the cell capable of enduring the stress and delaying the apoptotic cascades. If the stress can be removed, the cell may survive. However, if the stress is not eliminated, once a point of no return is reached, the addition of antioxidant is no longer able to prevent apoptosis. From Figure 6(B), we can see that to provide effective protection, pretreatment of NAC before arsenite insult is needed, as this prevents the possible diverse signal transduction cascades exerted by arsenite (since more than one factor may mediate the process of apoptosis). When NAC and arsenite were added at the same time, the small increase in cell apoptosis indicated that some cascade had already been triggered, which caused cell death. HSPs are immediately induced when cells receive insults, and function at early time points to protect the cells against the harmful effect of oxidative stress.

In conclusion, we have documented the first proteomic study on LECs and demonstrated that a high level (40 μM) of arsenite causes oxidative stress-induced apoptosis. This is supported by the fact that the free radical scavenger NAC effectively prevents cell death and the induction of HSPs is also abrogated. Western-blot analyses demonstrated that pretreatment with 20 mM NAC or GSH effectively suppressed the Bax expression and procaspase 3 activation in LECs treated with 40 μM arsenite. Our results indicate that treatment with 40 μM arsenite caused oxidative stress and subsequently up-regulated stress proteins, which served to protect the cells from apoptosis. Our ongoing studies aim to delineate the signalling pathway responsible for the regulation of these defence proteins and will hopefully provide more insights into this area in the future.

This work was partially supported by seed funding from the University of Hong Kong (10204004/39815/43700/301/01 and 10204565/38181/25200/301/01), RGC grants (HKU2718/02M and HKU7395/03M) and the Areas of Excellence scheme of Hong Kong University Grants Committee. We thank Dr D. Wilmshurst for critical reading of the paper and Amersham Biosciences for technical information in 2-DE. We also thank J. F. Song, J. Chen and Cynthie Y. H. Cheung for MALDI–TOF-MS analysis and are grateful to Y. Zhou for two-dimensional gel image analysis and for technical assistance in our proteomic studies at the University of Hong Kong.

REFERENCES

1 Lau, A. T. and Chiu, J. F. (2003) Arsenic is a paradoxical toxic metal: carcinogen and anticarcinogenic agent. Recent Res. Dev. Cell. Biochem. **1**, 1–19
2 Steinmaus, C., Moore, L., Hopenhayn-Rich, C., Biggs, M. L. and Smith, A. H. (2000) Arsenic in drinking water and bladder cancer. Cancer Invest. **18**, 174–182
3 EPA (1988) Risk Assessment Forum. Special Report on Ingested Arsenic: Skin Cancer; Nutrition Essentiality. United States Environmental Protection Agency
4 International Agency for Research on Cancer (1987) IARC Monogr. Eval. Carcinog. Risks Hum., vol. 1–42 (Suppl. 7), pp. 100–106
5 Hamadeh, H. K., Vargas, M., Lee, E. and Menzel, D. B. (1999) Arsenic disrupts cellular levels of p53 and mdm2: a potential mechanism of carcinogenesis. Biochem. Biophys. Res. Commun. **263**, 446–449
6 Kitchin, K. T. (2001) Recent advances in arsenic carcinogenesis: modes of action, animal model systems, and methylated arsenic metabolites. Toxicol. Appl. Pharmacol. **172**, 249–261
7 Gonsebatt, M. E., Vega, L., Salazar, A. M., Montero, R., Guzman, P., Blas, J., Del Razo, L. M., Garcia-Vargas, G., Albores, A., Cebrian, M. E. et al. (1997) Cytogenetic effects in human exposure to arsenic. Mutat. Res. **386**, 219–228
8 Barrett, J. C., Lamb, P. W., Wang, T. C. and Lee, T. C. (1989) Mechanisms of arsenic-induced cell transformation. Biol. Trace Elem. Res. **21**, 421–429
9 Nakamuro, K. and Sayato, Y. (1981) Comparative studies of chromosomal aberration induced by trivalent and pentavalent arsenic. Mutat. Res. **88**, 73–80
10 Chou, W. C., Hawkins, A. L., Barrett, J. F., Griffin, C. A. and Dang, C. V. (2001) Arsenic inhibition of telomerase transcription leads to genetic instability. J. Clin. Invest. **108**, 1541–1547
11 Lee-Chen, S. F., Yu, C. T. and Jan, K. Y. (1992) Effect of arsenite on the DNA repair of UV-irradiated Chinese hamster ovary cells. Mutagenesis **7**, 51–55
12 Lynn, S., Lai, H. T., Gurr, J. R. and Jan, K. Y. (1997) Arsenite retards DNA break rejoining by inhibiting DNA ligation. Mutagenesis **12**, 353–358
13 Wang, T. S., Hsu, T. Y., Chung, C. H., Wang, A. S., Bau, D. T. and Jan, K. Y. (2001) Arsenite induces oxidative DNA adducts and DNA–protein cross-links in mammalian cells. Free Radical Biol. Med. **31**, 321–330
14 Cavigelli, M., Li, W. W., Lin, A., Su, B., Yoshioka, K. and Karin, M. (1996) The tumor promoter arsenite stimulates AP-1 activity by inhibiting a JNK phosphatase. EMBO J. **15**, 6269–6279
15 Samet, J. M., Graves, L. M., Quay, J., Dailey, L. A., Devlin, R. B., Ghio, A. J., Wu, W., Bromberg, P. A. and Reed, W. (1998) Activation of MAPKs in human bronchial epithelial cells exposed to metals. Am. J. Physiol. **275**, L551–L558
16 Wu, W., Graves, L. M., Jaspers, I., Devlin, R. B., Reed, W. and Samet, J. M. (1999) Activation of the EGF receptor signaling pathway in human airway epithelial cells exposed to metals. Am. J. Physiol. **277**, L924–L931
17 Matsui, M., Nishigori, C., Toyokuni, S., Takada, J., Akaboshi, M., Ishikawa, M., Imamura, S. and Miyachi, Y. (1999) The role of oxidative DNA damage in human arsenic carcinogenesis: detection of 8-hydroxy-2′-deoxyguanosine in arsenic-related Bowen's disease. J. Invest. Dermatol. **113**, 26–31
18 Zhu, X. H., Shen, Y. L., Jing, Y. K., Cai, X., Jia, P. M., Huang, Y., Tang, W., Shi, G. Y., Sun, Y. P., Dai, J. et al. (1999) Apoptosis and growth inhibition in malignant lymphocytes after treatment with arsenic trioxide at clinically achievable concentrations. J. Natl. Cancer Inst. **91**, 772–778
19 Zhu, J., Chen, Z., Lallemand-Breitenbach, V. and De The, H. (2002) How acute promyelocytic leukaemia revived arsenic. Nat. Rev. Cancer **2**, 705–714
20 Gurr, J. R., Bau, D. T., Liu, F., Lynn, S. and Jan, K. Y. (1999) Dithiothreitol enhances arsenic trioxide-induced apoptosis in NB4 cells. Mol. Pharmacol. **56**, 102–109
21 Lau, A. T., Li, M., Xie, R., He, Q. Y. and Chiu, J. F. (2004) Opposed arsenite-induced signaling pathways promote cell proliferation or apoptosis in cultured lung cells. Carcinogenesis **25**, 21–28
22 Liu, L., Trimarchi, J. R., Navarro, P., Blasco, M. A. and Keefe, D. L. (2003) Oxidative stress contributes to arsenic-induced telomere attrition, chromosome instability, and apoptosis. J. Biol. Chem. **278**, 31998–32004
23 Bernstam, L. and Nriagu, J. (2000) Molecular aspects of arsenic stress. J. Toxicol. Environ. Health B Crit. Rev. **3**, 293–322
24 Li, M., Cai, J. F. and Chiu, J. F. (2002) Arsenic induces oxidative stress and activates stress gene expressions in cultured lung epithelial cells. J. Cell. Biochem. **87**, 29–38
25 Lau, A. T., He, Q. Y. and Chiu, J. F. (2003) Proteomic technology and its biomedical applications. Acta Biochim. Biophys. Sin. **35**, 965–975
26 Jungblut, P. R., Zimny-Arndt, U., Zeindl-Eberhart, E., Stulik, J., Koupilova, K., Pleissner, K. P., Otto, A., Muller, E. C., Sokolowska-Kohler, W., Grabher, G. et al. (1999) Proteomics in human disease: cancer, heart and infectious diseases. Electrophoresis **20**, 2100–2110
27 Hanash, S. M., Madoz-Gurpide, J. and Misek, D. E. (2002) Identification of novel targets for cancer therapy using expression proteomics. Leukemia **16**, 478–485
28 Bradford, M. M. (1976) A rapid and sensitive method for the quantitation of microgram quantities of protein utilizing the principle of protein–dye binding. Anal. Biochem. **72**, 248–254
29 Huang, H., Huang, C. F., Wu, D. R., Jinn, C. M. and Jan, K. Y. (1993) Glutathione as a cellular defence against arsenite toxicity in cultured Chinese hamster ovary cells. Toxicology **79**, 195–204
30 Schlesinger, M. J. (1990) Heat shock proteins. J. Biol. Chem. **265**, 12111–12114
31 Welsh, M. J. and Gaestel, M. (1998) Small heat-shock protein family: function in health and disease. Ann. N. Y. Acad. Sci. **851**, 28–35
32 Ito, H., Kamei, K., Iwamoto, I., Inaguma, Y., Nohara, D. and Kato, K. (2001) Phosphorylation-induced change of the oligomerization state of αB-crystallin. J. Biol. Chem. **276**, 5346–5352
33 Guay, J., Lambert, H., Gingras-Breton, G., Lavoie, J. N., Huot, J. and Landry, J. (1997) Regulation of actin filament dynamics by p38 map kinase-mediated phosphorylation of heat shock protein 27. J. Cell Sci. **110**, 357–368

34 Huot, J., Houle, F., Spitz, D. R. and Landry, J. (1996) HSP27 phosphorylation-mediated resistance against actin fragmentation and cell death induced by oxidative stress. Cancer Res. **56**, 273–279
35 Rane, M. J., Pan, Y., Singh, S., Powell, D. W., Wu, R., Cummins, T., Chen, Q., McLeish, K. R. and Klein, J. B. (2003) Heat shock protein 27 controls apoptosis by regulating Akt activation. J. Biol. Chem. **278**, 27828–27835
36 Garrido, C., Bruey, J. M., Fromentin, A., Hammann, A., Arrigo, A. P. and Solary, E. (1999) HSP27 inhibits cytochrome *c*-dependent activation of procaspase-9. FASEB J. **13**, 2061–2070
37 Kamradt, M. C., Chen, F. and Cryns, V. L. (2001) The small heat shock protein αB-crystallin negatively regulates cytochrome *c*- and caspase-8-dependent activation of caspase-3 by inhibiting its autoproteolytic maturation. J. Biol. Chem. **276**, 16059–16063
38 Arrigo, A. P. (1998) Small stress proteins: chaperones that act as regulators of intracellular redox state and programmed cell death. Biol. Chem. **379**, 19–26
39 Meriin, A. B., Yaglom, J. A., Gabai, V. L., Zon, L., Ganiatsas, S., Mosser, D. D., Zon, L. and Sherman, M. Y. (1999) Protein-damaging stresses activate c-Jun N-terminal kinase via inhibition of its dephosphorylation: a novel pathway controlled by HSP72. Mol. Cell. Biol. **19**, 2547–2555
40 Park, H. S., Lee, J. S., Huh, S. H., Seo, J. S. and Choi, E. J. (2001) Hsp72 functions as a natural inhibitory protein of c-Jun N-terminal kinase. EMBO J. **20**, 446–456
41 Mosser, D. D., Caron, A. W., Bourget, L., Meriin, A. B., Sherman, M. Y., Morimoto, R. I. and Massie, B. (2000) The chaperone function of hsp70 is required for protection against stress-induced apoptosis. Mol. Cell. Biol. **20**, 7146–7159
42 Creagh, E. M., Carmody, R. J. and Cotter, T. G. (2000) Heat shock protein 70 inhibits caspase-dependent and -independent apoptosis in Jurkat T cells. Exp. Cell Res. **257**, 58–66
43 Spycher, S. E., Tabataba-Vakili, S., O'Donnell, V. B., Palomba, L. and Azzi, A. (1997) Aldose reductase induction: a novel response to oxidative stress of smooth muscle cells. FASEB J. **11**, 181–188
44 Ewing, J. F. and Maines, M. D. (1991) Rapid induction of heme oxygenase 1 mRNA and protein by hyperthermia in rat brain: heme oxygenase 2 is not a heat shock protein. Proc. Natl. Acad. Sci. U.S.A. **88**, 5364–5368
45 Marilena, G. (1997) New physiological importance of two classic residual products: carbon monoxide and bilirubin. Biochem. Mol. Med. **61**, 136–142
46 Theil, E. C. (1987) Ferritin: structure, gene regulation, and cellular function in animals, plants, and microorganisms. Annu. Rev. Biochem. **56**, 289–315
47 Cairo, G., Tacchini, L., Pogliaghi, G., Anzon, E., Tomasi, A. and Bernelli-Zazzera, A. (1995) Induction of ferritin synthesis by oxidative stress. Transcriptional and post-transcriptional regulation by expansion of the 'free' iron pool. J. Biol. Chem. **270**, 700–703
48 Dastoor, Z. and Dreyer, J. L. (2001) Potential role of nuclear translocation of glyceraldehyde-3-phosphate dehydrogenase in apoptosis and oxidative stress. J. Cell Sci. **114**, 1643–1653

Received 10 February 2004/10 May 2004; accepted 3 June 2004
Published as BJ Immediate Publication 3 June 2004, DOI 10.1042/BJ20040224